Advances in Computational Design, *Vol. 1, No. 3 (2016) 253-264*
DOI: http://dx.doi.org/10.12989/acd.2016.1.3.253

Determination of strut efficiency factor for concrete deep beams with and without fibre

Sandeep M.S.*, Praveen Nagarajan[a], A.P. Shashikala[b] and Shehin A. Habeeb[c]

Department of Civil Engineering, NIT Calicut

(Received January 10, 2016, Revised June 25, 2016, Accepted June 28, 2016)

Abstract. Based on the variation of strain along the cross section, any region in a structural member can be classified into two regions namely, Bernoulli's region (B-region) and Disturbed region (D-region). Since the variation of strain along the cross section for a B-region is linear, well-developed theories are available for their analysis and design. On the other hand, the design of D-region is carried out based on thumb rules and past experience due to the presence of nonlinear strain distribution. Strut-and-Tie method is a novel approach that can be used for the analysis and design of both B-region as well as D-region with equal importance. The strut efficiency factor (β_s) is needed for the design and analysis of concrete members using Strut and Tie method. In this paper, equations for finding β_s for bottle shaped struts in concrete deep beams (a D-region) with and without steel fibres are developed. The effects of transverse reinforcement on β_s are also considered. Numerical studies using commercially available finite element software along with limited amount of experimental studies were used to find β_s.

Keywords: strut; efficiency factor; strut-and-tie; STM; fibre reinforced concrete; SFRC; ANSYS; nonlinear analysis of concrete; nonlinear finite element analysis of reinforced concrete

1. Introduction

Any region in a structure can be classified into two regions namely, Bernoulli's region (B-Region) and Disturbed region (D-Region) based on the variation of strain across the cross section. The well-developed flexure theories can be used for analysis and design B-Regions. On the contrary, due to the presence of nonlinear strain distribution the analysis and design of D-region is carried out based on thumb rules and past experience. Since both the B-region as well as D-region of a structure are of equal importance, a method that can be used for designing both the regions with equal importance is needed. Strut-and-Tie method is an alternative approach that can be used for the analysis and design of a structure providing equal importance for B-region and D-region. This method has found place in many of the international codes like American code ACI-318-14, Canadian code CSA-A23.3-14, Australian code AS 3600-2009, Euro code EC2:2004, New

*Corresponding author, Research Scholar, E-mail: sandeep.ms1986@gmail.com
[a]Associate Professor, E-mail: praveen@nitc.ac.in
[b]Professor
[c]M-Tech student

http://www.techno-press.com/journals/acd&subpage=7 ISSN: 2383-8477 (Print), 2466-0523 (Online)

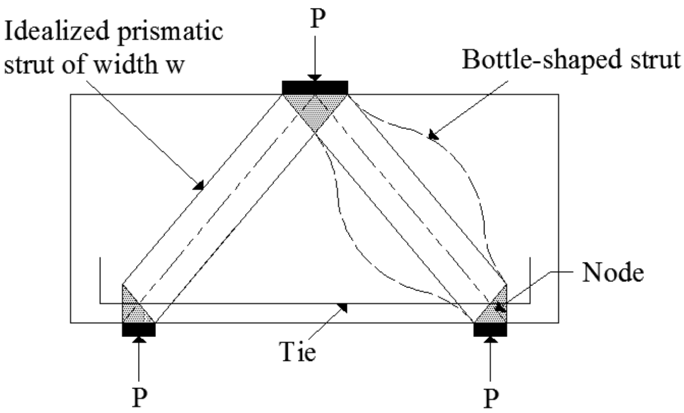

Fig. 1 STM for deep beam with central point load

Zealand code NZE 3101-1-2006, etc. A strut-and-tie model (STM) mainly consist of three parts which are compression struts, tension ties and nodes. The struts are members of a strut-and-tie model that carry compression force and the ties are members that carry tensile force. The intersection portion of members of a strut-and-tie model are termed as nodes. Fig. 1 illustrates the different components of a STM for a deep beam.

The accurate estimation of the strength of concrete strut is the key to the effectiveness of strut-and-tie method. The major type of strut that are commonly used are prismatic or bottle-shaped, depending on their positions within the structural element. The cross sectional area of a prismatic strut is uniform over its entire length whereas in a bottle-shaped strut, the cross-sectional area increases towards the mid-length with the strut assuming a bottle- shaped profile owing to lateral spreading of the compressive stress field. Even though reasonable amount of research has been carried out to establish the allowable strength of a strut for normal concrete, the work done on the allowable strength of fibre reinforced concrete is less. STM procedures were introduced in the 2002 version of American Concrete Institute (ACI) 318 as ‘Appendix A: Strut-and-tie Model’s, which underwent minor changes in the later versions. In chapter 23 of ACI 318-14, the nominal compressive strength of a strut is given by Eq. (1)

$$F_{ns} = f_{ce} A_{cs} \tag{1}$$

[Eq. 23.4.1a, ACI 318-14 chapter 23]

Where F_{ns} is nominal compressive strength of a strut without longitudinal reinforcement, A_{cs} is the lesser of the cross-sectional areas at the two ends of a strut, f_{ce} is effective compressive strength of concrete in the strut taken as the smaller of the two values obtained from Eqs. (2) and (3)

$$f_{ce} = 0.85\, \beta_s\, f_c' \tag{2}$$

[Eq. 23.4.3, ACI 318-14 chapter 23]

Where β_s is the ACI strut efficiency factor given in Table 1 and f_c' is the cylinder compressive strength of concrete

$$f_{ce} = 0.85\, \beta_n\, f_c' \tag{3}$$

[Eq. 23.9.2, ACI 318-14 chapter 23]

Table 1 Efficiency factors for struts as per ACI 318-14

Type of strut	**Efficiency Factor β_s**
Prismatic strut (uniform cross-sectional area)	1.00
Bottle-shaped strut with at least 0.3% effective transverse reinforcement	0.75
Bottle-shaped strut without or less than 0.3% reinforcement	0.60 λ
Struts in tension members or tension flanges of members	0.40
Struts in all other cases	0.60λ

Note: λ=1 for normal-weight concrete; 0.85 for sand lightweight concrete; 0.75 for all lightweight concrete

Where, β_n is the nodal efficiency factor taken as 1.00 for CCC nodes, 0.80 for CCT nodes and 0.60 for CTT as well as TTT nodes in accordance with Table 23.9.2 of ACI318-14. In the ACI node designation mentioned above, the letters 'C' and 'T' stand for 'compression' and 'tension', respectively.

The minimum amount of web reinforcement required is obtained using Eq. (4)

$$\sum \frac{A_{si}}{b_s s_i} sin\alpha_i \geq 0.003 \tag{4}$$

[Eq. 23.5.3, ACI 318-14 chapter 23]

Where A_{si} is the total area of distributed reinforcement at spacing s_i in the i-th direction of reinforcement crossing a strut at an angle α_i to the axis of a strut, and b_s is the width of the strut.

Brown *et al*. (2006) have observed that the amount of reinforcement required in a strut calculated using the ACI expression produced conservative but unpredictable results when compared with the test data. Further, Quintero-Febres *et al*. (2006) have found inconsistencies in the provisions for minimum reinforcement crossing a strut in sections A.3.3 and A.3.3.1 when applied to the test specimens. It was found that the former lead to substantially larger reinforcement ratios. The use of a strut efficiency factor β_s=0.60 in high-strength concrete bottle-shaped struts without web reinforcement led to strength predictions approximately 10% higher than the experimental failure loads. The higher strength recommended by Schlaich and Schäfer (1987) for prismatic struts, which presumably forms the basis for the ACI recommendations, is based on the assumption that prismatic struts are typical of B-regions and these recommendations may not hold good for prismatic struts located in D-regions wherein a more complex force system prevails. Further Sahoo *et al*. (2008) have noticed in their investigation that a bottle-shaped strut is in no way inferior to a prismatic strut in terms of strength and also suggested that the efficiency factor of bottle-shaped struts needs to be revised.

The popularity of steel fibre reinforce concrete (SFRC) construction is increasing day by day. The use of steel fibres helps in reducing the amount of conventional reinforcement required and there by reduces the complicated detailing requirements and the congestions of reinforcements, especially in beam column joints. SFRC members provided better ductile behavior, shear strength and reduced crack width compared to normal concrete Dupont and Vandewalle (2003). The strength, deformation capacities and crack control for deep beams were found to be improved by the addition of steel fibre to normal concrete Narayanan and Darwish (1988), Mansur and Ong (1991).

The aim of the present study was to check the effectiveness of efficiency factor proposed by ACI 318-14 for the analysis and design of reinforced concrete deep beams using STM method and to study the effect of steel fibre on the strut efficiency factor of concrete deep beams. For this, limited experimental and numerical study were conducted on deep beams. From the ultimate load capacity obtained, the efficiency factor for the struts were found out and the same were compared with the values provided in ACI-318-14.

2. Nonlinear finite element analysis using ANSYS

In the present study Solid65 element, available in ANSYS element library, was used to model concrete. Solid65 elements have elements node with three degrees of freedom at each of these nodes (translations in the nodal x, y, and z directions). The element is capable of plastic deformation, cracking in three orthogonal directions, and crushing. This element has inbuilt capability of modeling rebar in specific orientation. Whenever the rebar capability of solid65 is used, reinforcement is assumed to be smeared throughout the element in the provided orientation. In this work, this feature of solid65 element was utilized to model the steel fibre reinforcement in concrete. In the present study for modelling discrete reinforcement in the concrete volume, Link180 which is an element having two nodes with three degrees of freedom at each node, was used. This element is also capable of plastic deformation. A typical representation showing the geometry and node locations for these element types are shown in Figs. 2(a)-(b).

An eight-node solid element, Solid185, was used for the steel plates at support and load locations. The element is defined with eight nodes having three degrees of freedom at each node and translations in the nodal x, y, and z directions. Steel plate modelled using Solid185 elements, was added at the support locations in order to avoid stress concentration problems and to prevent localized crushing of concrete elements near the supporting points and location at which load is applied. A typical representation showing the geometry and node locations for this element type is shown in Fig. 3.

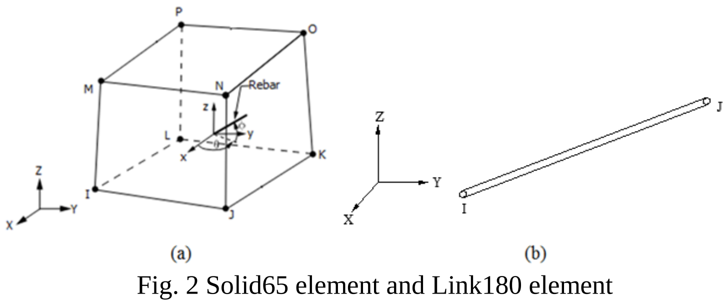

Fig. 2 Solid65 element and Link180 element

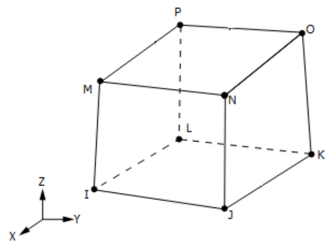

Fig. 3 Solid185 element

The Solid65 element requires linear isotropic and multi-linear isotropic material properties to properly model concrete. The multi-linear isotropic material uses the von Mises failure criterion along with the Willam and Warnke (1975) model to define the failure surface of concrete. The compressive uniaxial stress-strain relationship for the concrete model was obtained using Eq. (5) Hayder and Kamonna (2010). The stress-strain relation for the steel was defined using a bilinear curve with a yield stress of 415 MPa

$$f = \frac{E_c \times \varepsilon}{1 + \left(\frac{\varepsilon}{\varepsilon_o}\right)^2} \tag{5}$$

$$\varepsilon_o = \frac{2f_c'}{1 + \left(\frac{\varepsilon}{\varepsilon_o}\right)^2} \tag{5a}$$

$$E_c = \frac{f}{\varepsilon} \tag{5b}$$

Where:
f=stress at any strain ε, N/mm^2
ε_o=strain at ultimate compressive strength, f_c'

3. Experimental program for validation of finite element analysis

Four concrete deep beams with and without steel fibre were cast and tested for validating the results of analysis using ANSYS. The typical dimensions and reinforcement details of the tested beams are shown in Fig. 4. The deep beam specimens were designated as E1 to E4 as shown in Table 2. Specimen E1 and E2 were reference specimen with 0% steel fibre and the remaining two specimens E3 and E4 were steel fibre reinforced concrete specimens. All the beams were designed using the equations developed by Nagarajan P and Pillai T. M. M (2008) to ensure shear mode of failure. The mix proportion used for casting the deep beam was 1:1.5:3. For obtaining the 28th day compressive strength of concrete, three cubes of standard dimensions were cast and compacted by the standard methods. The effective span of the beam was 540 mm and the effective depth was 325 mm with an effective cover of 25 mm for the main tension steel of 16 mm diameter. Crack control

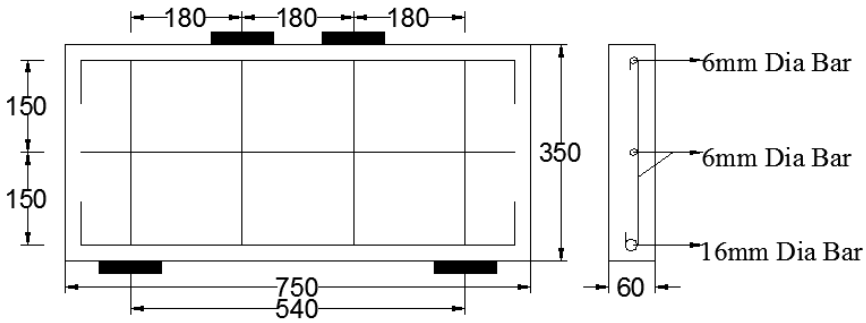

Fig. 4 Typical reinforcement details of deep beam

reinforcement was designed based on ACI 318-2014 and bars of 6 mm diameter were used to form the horizontal and vertical reinforcement for all the beams.

The beams were tested in a compression and bending testing machine. The load was started from 0 and was increased gradually till failure. A dial gauge was fixed right at the middle on the bottom face to measure the deflection of the beam and the readings were taken at regular load intervals. The test set-up is shown in Fig. 5. The results of all the tested beams are shown in Table 2. A comparison of failure load obtained by experiment and numerical analysis is also presented in Table 2. The Load-Deflection curves showing the experimental results as well as the results obtained by carrying out the non-linear finite element analysis using ANSYS for beams E1 to E4 are shown in Figs. (6)-(9). The crack pattern obtained for beams E1 experimentally and that obtained from ANSYS is shown in Figs. 10(a)-(b).

Table 2 Test results of beams E1 to E4

No	Specimen	Steel Fibre Content (%)	Compressive Strength (MPa)	Failure Load (Experimental) (MPa)	Failure Load (Numerical) (MPa)	Percentage Difference in Failure Load
1	E1	0	35.83	127.53	149.00	14.40%
2	E2	0	35.83	130.00	149.00	12.75%
3	E3	0.75	37.63	191.30	215.00	11.00%
4	E4	1	38.23	191.30	216.00	11.44%

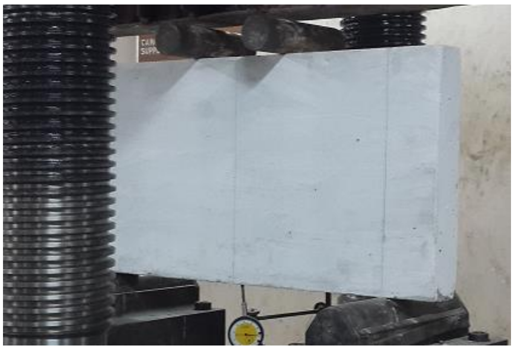

Fig. 5 Test set-up

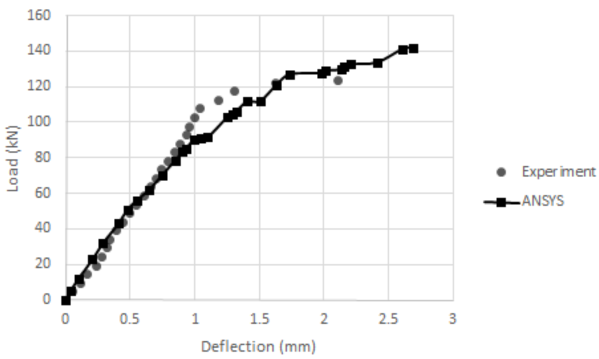

Fig. 6 Load Deflection Plot for Beam E1

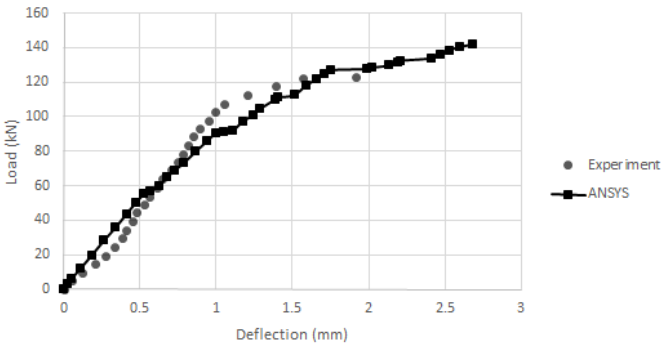

Fig. 7 Load Deflection Plot for Beam E2

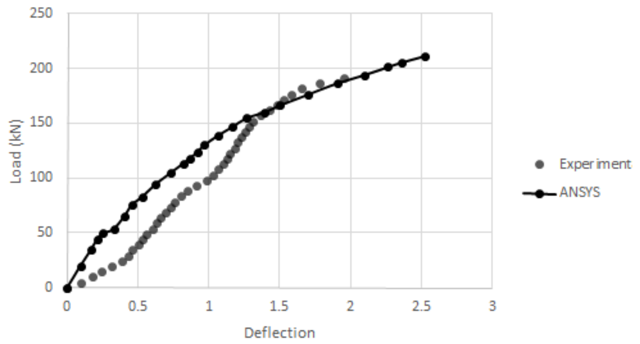

Fig. 8 Load deflection plot for beam E3

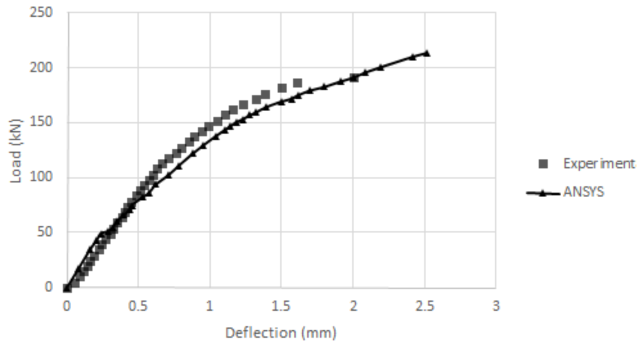

Fig. 9 Load deflection plot for beam E4

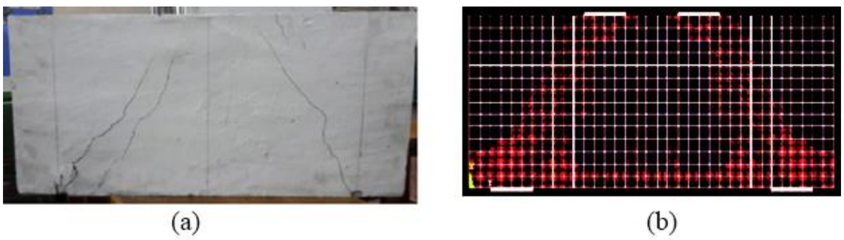

Fig. 10 Crack pattern for beam E1 (a) From Experiment (b) From ANSYS

The results obtained from the numerical analysis was showing good agreement with those obtained from the experiment.

4. Determination of strut efficiency factor from collapse load of deep beam

From the collapse load obtained from the experimental/numerical study, the strut efficiency factor can be calculated as explained below. The typical STM used for the calculation is shown in Fig. 11.

The dimensions of the beam are same as that shown in Fig. 4. From Fig. 11, the least lateral dimension, W_s, of the bottle-shaped strut that could be formed between the support and at the point where load is applied is obtained at its interface with node A

$$W_s = W_t \cos\theta + L_b \sin\theta \quad (6)$$

Where 'θ' is the angle between the tension tie and the axis of the bottle shaped strut as shown in Fig. 11

$\theta = tan^{-1} (\frac{300}{180}) = 59.036^o$

W_s = 50 *cos* (59.036) + 30 *sin* (59.036) = 51.45 mm

As the beam thickness, *b,* is 60 mm, the least cross-sectional area of the bottle-shaped strut is:

A_{cs} = 60 *A*? 51.45 = 3086.98 mm^2

From statics, since the beam is symmetric, the reaction at both the support is half of the applied load *P*. The axial force in the strut can therefore be expressed in terms of the peak load, P_u.

Force in strut, $F = \frac{0.5 \times P_u}{sin\,(59.036)} = 0.583\ P_u.s$

Therefore, in Eq. (1), F_{ns} can be replaced by F and the strut efficiency factor, β_s, can be computed combining Eqs. (1) and (2) as

$$\beta_s = \frac{0.583\ P_u}{(0.85\ f_c'\ A_{cs})} \quad (7)$$

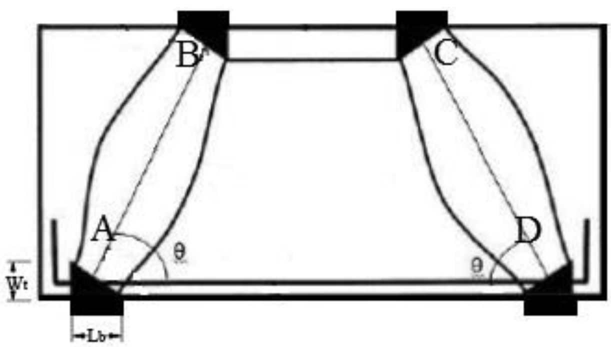

Fig. 11 Typical STM for deep beam

Table 3 Strut efficiency factor from collapse load for beams E1 to E4

Specimen	Compressive Strength (MPa)	Ultimate Load (kN)	Strut Efficiency Factor (β_s)
E1	35.83	127.53	0.99
E2	35.83	130.00	1.00
E3	39.90	191.30	1.33
E4	36.08	191.30	1.47

Using Eq. (7) strut efficiency factor for all the beams used for validating the results of analysis in ANSYS, was calculated from the collapse load. The calculated strut efficiency factor for beams E1 to E4 are tabulated in Table 3.

5. Numerical analysis of deep beams using ANSYS

Since there was good agreement between the results obtained using experimental and numerical analysis, a number of beams, with specimen designated from A1 to A6 as shown in Table 4, were modelled and analyzed in ANSYS. All the beams were of size 750 mm *A*? 350 mm *A*? 60 mm. The beams were designed to ensure shear mode of failure. Typical reinforcement details of the beams are shown in Fig. 4. Non-linear Finite Element analysis was carried out for beams A1 to A6 with different ratios of horizontal and vertical reinforcement. Symmetric two-point loading was applied for the model. For beam A1 the horizontal and vertical mesh of reinforcements were spaced at 50 mm c/c. The diameter of the bars was 6 mm. First, the vertical reinforcement spacing was increased for the beams keeping the horizontal reinforcement spacing a constant. The non-linear analysis was then carried out and the failure loads and the central deflection were recorded. Then the models were analyzed by varying the horizontal reinforcement spacing, keeping the vertical reinforcement spacing a constant. Corresponding failure load and load deflection data were noted. The failure load and final deflection for beams A1 to A6 are shown in Table 4.

Table 4 Failure load and central deflection for beams A1 to A6

No	Specimen	Horizontal Reinforcement Spacing (mm)	Vertical Reinforcement Spacing (mm)	Horizontal Reinforcement Percentage	Vertical Reinforcement Percentage	Failure Load (kN)	Maximum Deflection (mm)
1	A1	50	50	0.01508	0.01508	248.80	1.07
2	A2	50	100	0.01508	0.00754	242.40	1.07
3	A3	50	150	0.01508	0.00503	236.80	1.30
4	A4	50	200	0.1508	0.00377	225.74	1.39
5	A5	100	50	0.00754	0.01508	232.00	1.20
6	A6	150	50	0.00503	0.01508	217.60	1.32

From Table 4, it was found that for deep beams with low shear span to depth ratio, the effect of horizontal web reinforcement on the ultimate shear capacity was more when compared to the effect of vertical web reinforcement.

To study the effect of steel fibre reinforcement on strut efficiency factor, steel fibre reinforced deep beams, with specimens designated as S1 to S10, having fibre content varying from 0% to 1%, at an interval of 0.25%, were modeled in ANSYS. The dimensions of these beams were same as that shown in Fig. 4. One 16 mm diameter bar was provided as the main tension reinforcement and 6 mm diameter bars were provide at 150 mm and 180 mm for horizontal and vertical web reinforcement respectively. The beams were analyzed under symmetric two-point loading. The strut efficiency factor for these beams were calculated using Eq. (7) and are tabulated in Table 5. In comparison to the values of strut efficiency factor for normal concrete, provided in ACI-318-14, analyzed steel fibre reinforced deep beam specimens were having higher strut efficiency factor.

Finally, an attempt was made to derive a relation between efficiency factor and steel fibre content. A plot was drawn between the efficiency factor calculated based on the results of

Table 5 Failure load and strut efficiency factor for beams S1 to S10

No	Specimen	Steel fibre Volume (%)	Failure Load (kN)	f_{ck} (MPa)	β_s
1	S1	0	150.00	35.825	1.16
2	S2	0.15	163.00	36.125	1.26
3	S3	0.25	173.53	36.425	1.32
4	S4	0.35	183.50	36.625	1.39
5	S5	0.45	191.00	36.825	1.44
6	S6	0.5	195.31	37.025	1.46
7	S7	0.65	207.00	37.325	1.54
8	S8	0.75	215.00	37.625	1.59
9	S9	0.85	215.55	37.825	1.58
10	S10	1	216.00	38.225	1.57

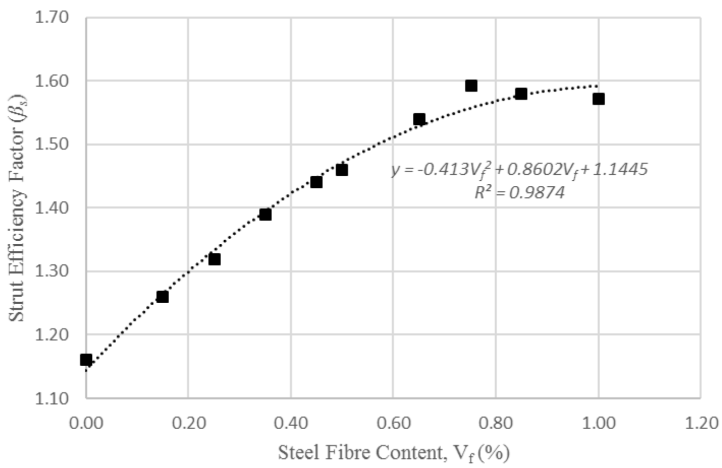

Fig. 12 Plot showing variation of efficiency factor with steel fibre ratio

numerical analysis and the steel fibre content which is shown in Fig. 12. It can be seen from Table 5 that as the ratio of steel fibre increases, the strut efficiency factor also increases. It can be also observed that beyond a steel fibre percentage of 0.75, there was no significant improvement in the load carrying capacity. So 0.75% can be considered as the optimum steel fibre content.

From Fig. 12, an equation (Eq. (8)) was developed for representing the variation of strength modification factor with respect to the steel fibre content where V_f stands for the steel fibre content by volume in percentage in the concrete matrix

$$\beta_s = -0.413V_f^{\,2} + 0.8602V_f + 1.1445 \tag{8}$$

Based on the study conducted it is found that the strut efficiency factor provided in ACI318-14 is on the conservative side.

6. Conclusions

An attempt was made to check the effectiveness of efficiency factor proposed by ACI 318-14 for the analysis and design of reinforced concrete deep beams using STM method. It was found that for deep beams with low shear span to depth ratio, the horizontal web reinforcement was having more effect than the vertical web reinforcement on the ultimate shear capacity. Based on the study conducted, strut efficiency factor for bottle-shaped struts for ordinary reinforced concrete deep beams were found to be more than or equal to 1.0, in contrast to 0.75 given in ACI-318-14 for sufficiently reinforced bottle shaped strut and 0.60 for unreinforced strut. In comparison to the strut efficiency factor provided in ACI 318-14, strut efficiency factor obtained for steel fibre reinforced concrete beams were higher. Based on the results of numerical analysis conducted, an equation was developed for finding the value of efficiency factor with respect to the steel fibre content. More experimental results are needed to further validate the equation which are in progress.

References

ANSYS, Inc., *ANSYS Help*, Release 12.1, Documentation, Copyright 2006.

ACI 318-14 (2014), *Building code requirements for structural concrete and commentary*, American Concrete Institute, USA.

Andermatt, M.F. and Lubell, A.S. (2013b), “Strength modeling of concrete deep beams reinforced with internal fiber-reinforced polymer”, *ACI Struct. J.*, **110**(4), 595-605.

Bahen, N. and Sanders, D.H. (2009), “Investigation of strut strength using a deep-beam database”, *ACI Struct. J.*, **SP-265**(18), 385-404.

Birrcher, D.B., Tuchscherer, R.G., Huizinga, M. and Bayrak, O. (2013), “Minimum web reinforcement in deep beams”, *ACI Struct. J.*, **110**(2), 297-306.

Brown, Michael, D., Sankovich, Cameron, L., Bayrak, Oguzhan and Jirsa, James, O. (2006), “Behavior and efficiency of bottle- shaped struts”, *ACI Struct. J.*, **103**(3), 348-355.

Chetchotisak, P., Teerawong, J. and Chetchotsak, D. (2014), “Efficiency factors for reinforced concrete deep beams: part 1 - improved models”, *Adv. Mater. Res.*, **931-932**, 506-513.

Chetchotisak, P., Teerawong, J. and Chetchotsak, D. (2014), “Efficiency factors for reinforced concrete deep beams: part2- code calibration”, *Adv. Mater. Res.*, **931-932**, 514-519.

Chetchotisak, P., Teerawong, J. and Yindeesuk, S. (2014), “New strut-and-tie-models for shear strength prediction and design of RC deep beams”, *Comput. Concrete*, **14**(1), 19-14.

Choi, H.B., Yi, C.K., Cho, H.H. and Kang, K.I. (2010), “Experimental study on the shear strength of recycled aggregate concrete beams”, *Magaz. Concrete Res.*, **62**(2), 103-114.

Dupont, D. and Vandewalle, L. (2003), “Shear capacity of concrete beams containing longitudinal reinforcement and steel fibers”, *Am. Concrete Inst. Spec. Pub.*, **216**, 79-94.

Hong, S. and Ha, T. (2012), “Effective capacity of diagonal strut for shear strength of reinforced concrete beams without shear reinforcement”, *ACI Struct. J.*, **109**(2), 139-148.

Hussein, Hayder, H. and Kamonna (2010), “Non-linear analysis of steel fibre reinforced concrete deep beams by ansys”, *Kufa J. Eng.*, **2**(1), 110-124.

Kim, D., Lee, J. and Lee, Y-H. (2014), “Effectiveness factor of strut-and-tie models for concrete deep beams reinforced with FRP rebars”, *Compos. Eng.: Part B*, **56**, 117-125.

Khan, M.A. and Ahmed, F.S. (2013), “Effect of web reinforcement on ultimate strength of reinforced concrete deep beam”, *Int. J. Eng. Res. Appl.*, **3**(3), 516-519.

Lihua, X.U., Yin, C.H.I., Jie, S.U. and Dongtao, X.I.A. (2008), “Nonlinear finite element analysis of steel fibre reinforced concrete deep beams”, *Wuhan Univ. J. Nat. Sci.*, **13**(2), 201-206.

Lu, W.Y., Hsiao, H.Tai., Chen, C.L., Huang, S.M. and Lin, M.C. (2015), “Tests of reinforced concrete deep beams”, *Comput. Concrete*, **15**(3), 357-372.

Mansur, M.A. and Ong, K.C.G. (1991), “Behavior of reinforced fibre concrete deep beams in shear”, *ACI Struct. J.*, **88**(1), 98-105.

Narayanan, R. and Darwish, I.Y.S. (1988), “Fibre concrete deep beams in shear”, *ACI Struct. J.*, **85**(2), 141-149.

Nagarajan, P. and Pillai, T.M.M. (2008), “Analysis and design of simply supported deep beams using strut and tie method”, *Adv. Struct. Eng.*, **11**(5), 491-499.

Nagarajan, P. and Pillai, T.M.M. (2008), “Development of strut and tie models for simply supported deep beams using topology optimisation”, *Songklanakarin J. Sci. Technol.*, **30**(5), 641-647.

Nagarajan, P. and Pillai, T.M.M. (2010), “Development of strut and tie models for continuous deep beams using topology optimisation”, *J. Struct. Eng.*, **37**(4), 81-85.

Nehdi, N., Omeman, Z. and EI-Chabib, H. (2008), “Optimal efficiency factor in strut-and-tie model for FRP-reinforced concrete short beams with ($1.5<a/d<2.5$)”, *Mater. Struct.*, **41**(10), 1713-1727.

Quntero-Febres, C.G., Parra-Montesinos, G. and Wight, J.K. (2006) “Strength of struts in deep concrete members designed using strut-and-tie method”, *ACI Struct. J.*, **103**(4), 577-586.

Sahoo, D.K., Singh, B. and Bhargava, P. (2009), “An appraisal of the ACI strut efficiency factors”, *Magaz. Concrete Res.*, **61**(6), 445-456.

Sahoo, D.K., Singh, B. and Bhargava, P. (2010), “Strut efficiency factors for structural concrete made from coarse recycled concrete aggregates”, *J. Struct. Eng.*, **37**(1), 49-54.

Sahoo, D.K., Singh, B. and Pradeep Bhargava (2011), “Minimum reinforcement for preventing splitting failure in bottle-shaped struts”, *ACI Struct. J.*, **108**(2), 206-216.

Sahoo, D.K., Flores, C.A. and Chao, Shih-Ho (2012), “Behavior of steel fibre-reinforced concrete deep beams with large opening”, *ACI Struct. J.*, **109**(2), 193-204.

Schlaich, J., Schäfer, K. and Jennewein, K. (1987), “Towards a consistent design of structural concrete”, *J. Prestress. Concrete Inst.*, **32**(3), 75-150.

Sclaich, J. and Schäfer, K. (1991), “Design and detailing of structural concrete using strut-and-tie models”, *Struct. Eng.*, **69**(6), 113-125.

Tuchscherer, R., Birrcher, D., Huizinga, M. and Bayrak, O. (2011), “Distribution of stirrups across web of deep beams”, *ACI Struct. J.*, **108**(1), 108-115.

Wolanski, A.J. (2004), “Flexural behaviour of reinforced and prestressed concrete beams using finite element analysis”, Master’s Dissertation, Marquette University, Milwaukee.